Influence of Wire-Connecting With Ni Electro-Plating on GMI Output Stability of Co-Rich Amorphous Microwires

Jing-Shun Liu[1,2], Da-Wei Xing[1], Da-Yue Zhang[3], Fu-Yang Cao[1], Xiang Xue[1], and Jian-Fei Sun[1]

[1]School of Materials Science and Engineering, Harbin Institute of Technology, Harbin 150001, China
[2]School of Materials Science and Engineering, Inner Mongolia University of Technology, Hohhot 010051, China
[3]School of Metallurgy and Materials, University of Birmingham, Edgbaston, Birmingham B15 2TT, U.K.

We present systematic studies on the effect of Ni electro-plated wire-connecting technique on giant magneto-impedance (GMI) output stability of melt-extracted amorphous CoFeSiB microwires for potential sensor applications. The electro-plated microstructure was observed by scanning electron microscopy (SEM) and the GMI output stability was characterized by a precision impedance analyzer and a magnetically shielded space. Experimental results indicated that Ni electro-plating (at 4.0 A/dm^2 for 230 s) caused the microwires to show homogeneous pyramid structures, better wettability and weldability, so improving the GMI output for reducing the RF wave emission and signal attenuation, minimizing the disturbance of stray capacity, and suppressing the destabilization and concussion at relatively high frequency, especially near RLC parallel resonance frequency, f_p. Moreover, the wire-connecting by Ni electro-plating could enhance the GMI output stability under different applied magnetic fields and frequencies. It can therefore be concluded that the microwires with Ni electro-plated two-terminal are suitable as stable GMI sources of high-resolution magnetic sensors.

***Index Terms*—Giant magneto-impedance (GMI) output stability, melt-extracted amorphous microwires, Ni electro-plating, wire-connecting.**

I. Introduction

AMORPHOUS magnetic microwires have attracted great interest from the research community recently. Such intensive studies are related with the potential industrial applications as magnetic- and stress-sensing sensor elements to detect weak magnetic fields in the car industry, biomedicine and navigation fields [1]–[7]. Especially for the weak giant magneto-impedance (GMI) and giant stress impedance (GSI) sensors, researchers tend to enhance their stability, precision, repeatability and linearity by improving the stability of impedance variation, namely, the impedance value of wire influenced by some interference factors can be certainly changed to some extent as the increase or decrease of magnetic field and frequency, and optimizing the design of electrical circuit (EC) and electronic package (EP). So that, even a slight fluctuation of impedance could be detected by further amplification circuit. Therefore, study on stability and reliability of such advanced microelectronic measurement devices has become more and more necessary [8]–[10]. Nevertheless, GMI output stability is confined by a certain number of restrictions, such as ambient temperature variation, electronic noise and external applied magnetic field, especially wire-connecting mode and contact instability of wire-connecting probes (namely pan welds) are of most important.

Therefore, for the melt-extracted amorphous microwires, it is very challenging to achieve a stable or reliable electrical interconnection between wire-terminal and solder used in microelectronic circuit in EP, but little effort has been given in the wire-connecting perspective [11]–[13]. The issue can be tackled from the following two aspects: 1) to seek for novel wire-connecting by electro-plating technique (a metallurgical welding process) of improving wetting characteristic of wire-terminal surface [14]; and 2) to assure the coefficient matching of thermal expansion (CTE) at certain value between nickel plating layer and microwire. Nickel electro-plating, with relatively low thermal expansion coefficient and good wettability, high electrical conductivity and stability in atmosphere, is a novel way to ensure the bondability and reliability in wire-connecting process applied for EP of chips with wire interconnections [11]. In our previous report, we employed Cu electro-plating to improve the wettability and bondability, also achieved the stable wire-connection at room temperature [11]. Once the ambient temperature changes, the mismatch of CTE between microwire (lower CTE, 7.28×10^{-6} K^{-1}) and Cu electroplated layer (higher CTE, 12.7×10^{-6} K^{-1}) also can result in stability of connection and GMI output stability. Thereby, from the matching perspective of CTE, we attempted to solve wire-connecting problem by the novel Ni electro-plating method (lower CTE comparing with Cu, 9.45×10^{-6} K^{-1}) in GMI sensor with amorphous microwires as sensing element and expect to stabilize impedance output in relatively broader frequency and magnetic field, including higher working temperature.

This paper aims to achieve a stable interconnection between Co-rich melt-extracted amorphous microwires and solder by properly controlling Ni electro-plating parameters at wire-terminal, and obtain the best conditions to maximize the GMI output stability. The results presented here are useful for fabricating high-performance GMI and GSI sensors.

II. Experimental Details

Soft magnetic amorphous microwire with nominal composition of $Co_{68.2}Fe_{4.3}B_{15}Si_{12.5}$ (in at. %) with diameter, $d =$

Manuscript received February 01, 2012; revised March 31, 2012, May 18, 2012, and July 02, 2012; accepted July 24, 2012. Date of publication August 07, 2012; date of current version November 20, 2013. Corresponding author: J.-S. Liu (e-mail: jingshun_liu@163.com; jingshun.liu1@gmail.com; jfsun_hit@263.net).

Color versions of one or more of the figures in this paper are available online at http://ieeexplore.ieee.org.

Digital Object Identifier 10.1109/TMAG.2012.2212023

TABLE I
COMPOSITION OF IMPROVED ELECTROLYTE FOR NI ELECTRO-PLATING

Composition	Proportion	Other parameters
$NiSO_4$	300 g/ L	Anode: 99.9% hyperpure nickel
$NiC1_2$	50 g/ L	Current density of cathode: 4.0 A/dm^2
HBO_3	40 g/ L	Electro-plating source: dc 0-30 V, 2 A
$C_{12}H_{25}$-OSO_3Na	100 mg/ L	Temperature: 55 ± 0.5 °C

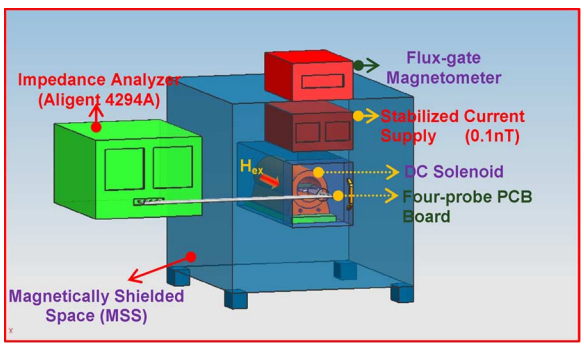

Fig. 1. Schematic illustrations of magneto-impedance measurement system and MSS. The uni-direction arrow represents the axial applied external magnetic field [16].

28.9 μm, was melt-extracted by the V-shaped edge of high-speed wheel of a precision melt-extraction facility filled with an argon atmosphere. The as-cast thin microwires possessed excellent soft magnetic properties owing to the vanishing or small negative magnetostriction constant ($|\lambda_s| \leq 3\times10^{-6}$). The samples with whole length of 24 mm of the two terminals (each about 4 mm long) were electro-plated by mini-type electro-plating device. The composition of improved nickel electro-plating electrolyte and related process parameters were listed in Table I, including nickel sulphate, nickel chloride, boric acid and lauryl sodium sulphate with proper proportion [15]. The added boric acid as the buffering agent is used to improve the surface quality of nickel layer and the bondability of electro-plated layer and substrate. While the lauryl sodium sulphate as wetting agent and surface active agent are propitious to reduce the boundary tension between electrode and solution, even decrease porosity of nickel layer.

The surface morphology of the electro-plated microwires was measured by scanning electron microscopy (SEM). Video-based contact angle measurement device (OCA 20LHT) was employed to measure the dynamic contact angles based on the analysis of the drop shape of the different types of interfaces in a pipe-still heater with 10^{-5} mbar vacuum. Fig. 1 illustrates the diagrammatic sketch of impedance measurement system and magnetically shielded space (MSS).

The magneto-impedance was measured by an Aligent 4294 A impedance analyzer in the frequency range of 40 Hz–110 MHz. The microwire with two-end electro-plated was connected into printed circuit board (PCB) adopting the four-probe method. The compositions of solder (SAC) were tin (96.5%), silver

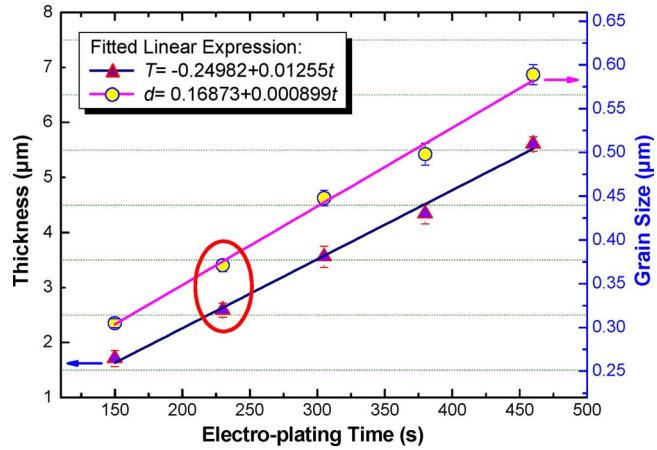

Fig. 2. Variation in thickness and grain size of Ni electro-plated layer and the corresponding fitted linears at the current density of 4.0 A/dm^2 for different electro-plating time from 150 to 460 s. The red ellipse indicates that the appropriate thickness and grain size of Ni electro-plated layer are the better state adopted.

(3.0%), and copper (0.5%), in weight percent, respectively. The magnetoimpedance ratio, $\Delta Z/Z_0$, is defined as [17]

$$\frac{\Delta Z}{Z_0}(\%) = \left[\frac{Z(H_{ex}) - Z(H_0)}{Z(H_0)}\right] \times 100\% \quad (1)$$

where the dc axial external magnetic field, $H_{\rm ex}$, is supplied by a solenoid and the maximum field along the wire axis up to $H_{\max}$ of 4.25 Oe, and $Z(H_0)$ is the initial impedance at $H_0 = 0$ Oe. All measurements were performed at room temperature (25 °C).

III. RESULTS AND DISCUSSION

Generally, the variation of impedance values can exhibit macroscopic fluctuant with increasing magnetic field at different frequency due to the poor wire-connecting, also including the electrical signal output. Therefore, we should solve the problem of stable wire-connecting at first in order to effectively evaluate the impedance and corresponding GMI output stability, and assure the impact of pan weld as little as possible. Importantly, it's necessary to investigate the effect of current density and electro-plating time on the microstructures evolution to determine the optimal parameters [18]. The amount of nickel deposited at the cathode and the amount dissolved at the anode are directly proportional to the current density and the electro-plating time given by the Faraday's Law (FL) [15]

$$m = 1.095aIt \quad (2)$$

where m is the weight amount of nickel deposited at the cathode (or dissolved at the anode); I is the current density; t is the electro-plating time; and a is the current efficiency ratio for the reaction of interest, $a \approx 0.95$ (in almost all cases). In the nickel electro-plating process at the current density of 4.0 A/dm^2, the thickness variation of electro-plated layer can be calculated by FL as, $T = 0.7832$ t. In practice, the average thickness measured at different positions and the average grain size estimated by Image-Pro-Plus software, both them with tiny error bars of the electro-plated nickel layer at the current density of 4.0 A/dm^2 are plotted in Fig. 2. The thickness of samples plated for 150, 230, 305, 380, and 460 s are about

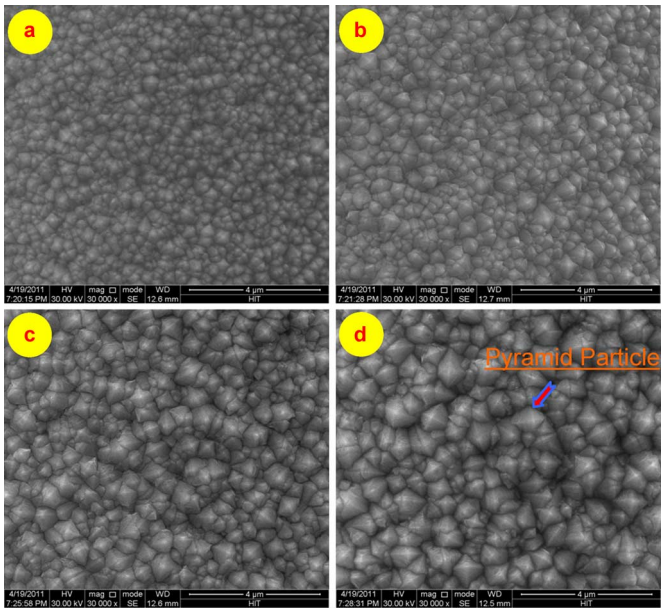

Fig. 3. SEM micrographs of microstructural evolution of Ni electro-plated layer at current density of 4.0 A/dm^2 for different electro-plating times: (a) 150 s, (b) 230 s, (c) 380 s, (d) 460 s, respectively.

1.71, 2.59, 3.56, 4.34, and 5.61 μm, respectively. The grain size plated for 150, 230, 305, 380, and 460 s are about 305, 361, 448, 498, and 589 nm, respectively. With an increase of electro-plating time from 150 to 460 s, the thickness and grain size of Ni layer increases linearly with plating time according to the following fitted relationships:

$$\begin{cases} T = -0.24982 + 0.01255\,t \\ d = 0.16873 + 0.000899\,t \end{cases} \tag{3}$$

where T is the thickness electro-plated nickel layer; d is grain size of electro-plated nickel particle; t is the electro-plating time. The thickness variation with increasing electro-plating time is slightly lower than the theoretical prediction by FL. So, we can calculate and control the electro-plating rate according to the above fitted expression (3) properly.

For the nickel electro-plating process, also is called Watt's nickel plating, the nickel layer is deposited in cathode (namely microwires) according to the following electro-chemical reactions [15]:

$$\text{Anode:} \quad \mathrm{Ni} - 2\mathrm{e}^- = \mathrm{Ni}^{2+} \tag{4}$$

$$\text{Cathode:} \quad \mathrm{Ni}^{2+} + 2\mathrm{e}^- = \mathrm{Ni}$$

$$2\mathrm{H}^+ + 2\mathrm{e}^- = \mathrm{H}_2\uparrow \quad \text{(Secondary Reaction)}. \tag{5}$$

Fig. 3 shows the SEM micrographs of microwires that underwent different times of Ni electro-plating at relatively high current density so high deposition rate. It shows that the longer electro-plating time caused the larger sized nickle particles parallel to the direction of layer thickness, coarser surface, consequently caused worse bondability between the nickel layer and the substrate. In general, the morphology evolution of nickel electro-plated layer consists of three stages, particle nucleation region (PNR) stage, particle growth region (PGR) stage and boundary layer region (BLR) as shown in Fig. 4.

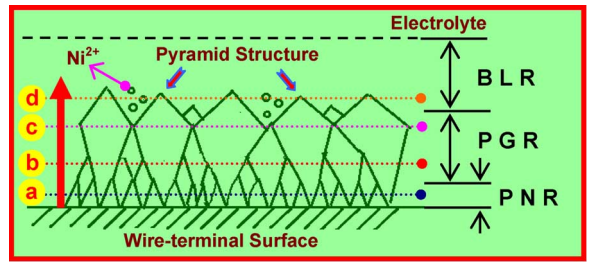

Fig. 4. Schematic diagrams of morphology evolution including three parts: particle nucleation region (PNR), particle growth region (PGR) and boundary layer region (BLR) on the amorphous wire-terminal surface for different time corresponding in Fig. 3(a)–(d).

At the beginning of PNR stage, the large quantity Ni^{2+} ion are deposited rapidly in terms of nucleuses on the wire-terminal surface, because of the uniform distribution of current density and the same Ni^{2+} ion concentration as electrolyte on the wire-terminal surface. For 150 s, Ni particles with small diameters are deposited on the wire-terminal surface at a relatively rapid plating rate, as shown in Fig. 3(a). For 230 s nickel particles are deposited densely and uniformly on the formed nucleuses, and then grow gradually with plating time increasing (also called PGR stage); finally the microstructure with smooth surface morphology and fine grain size is obtained, as shown in Fig. 3(b). While the plated layer surface becomes rougher and porous tendentiousness with the electro-plating time increasing to 380 s and further to 460 s, because of the formation of pyramid structure mainly composed by large-size grains and the generation of secondary reaction (mainly hydrogen liberation), as shown in Fig. 3(c) and (d). Meanwhile, with the nickel particle growing along some crystalline orientation, there is a tendency to forming nucleuses of new particles as the existence of the relatively high Ni^{2+} concentration gradient in the boundary layer between PGR and electrolyte, especially in the region of adjacent nickel particles, which is consistent with a previous report [14]. The size of new formed particle increases inhomogeneously since the action of different ion concentration gradients and hydrogen liberation reaction, so the uniformity and bondability of nickel plating layer decrease with the extending of electro-plating time, which is not suitable for final wire-connecting. In addition, the microwire Ni electro-plated at 4.0 A/dm^2 for 230 s also has smooth and uniform surface, and no serious plating defects, even has well rounded cross-section and clear interface between Ni layer and substrate [as seen in Fig. 5(a) and (b)]. During the final wire-connecting for impedance measurement and sensor application under different ambient temperature, Ni electro-plating layer exhibits excellent wettability (the contact angle of nickel layer and SAC is up to 54.60°, is smaller than the non electro-plating interface angle, 85.54°) and low coefficient of thermal expansion (the CTE value is around 9.45×10^{-6} K^{-1}). The relations between contact angles and interfaces for different connections are given in Fig. 5(d) and (e). Thus, we can obtain the suitable parameters (at current intensity of 4.0 A/dm^2 for 230 s) to control nickel electro-plating process at wire-terminal. Meanwhile, it means that excellent weldability between Ni electro-plated layers at wire-terminal and SAC solder is obtained by SAC/Ni

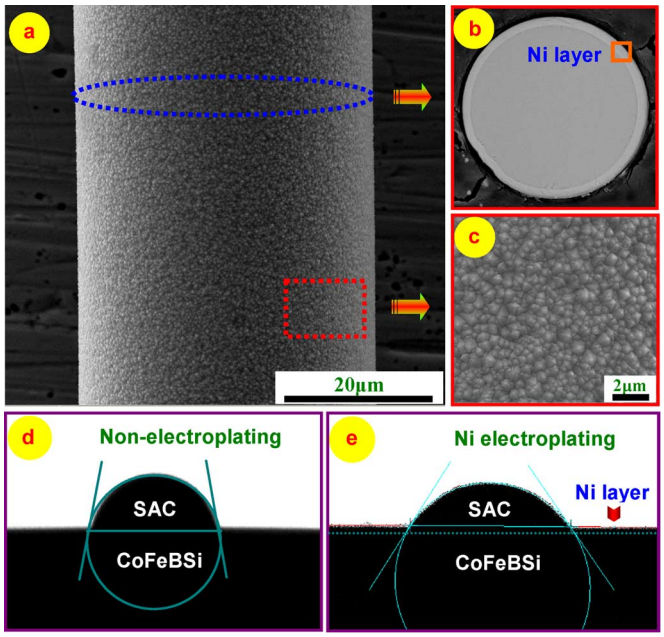

Fig. 5. SEM morphology of nickel electro-plated microwires at the current density of 4.0 A/dm^2 after electro-plating time of 230 s: (a) macroscopic surface; (b) cross-section; and (c) microscopic surface; and the wetting morphology of microwires with two typical interfaces: (d) nonelectro-plated interface and (e) Ni electro-plated interface. The OCA images (d) and (e) indicate contact angles of θ_d and θ_e are 85.54° [11] and 54.60°, respectively.

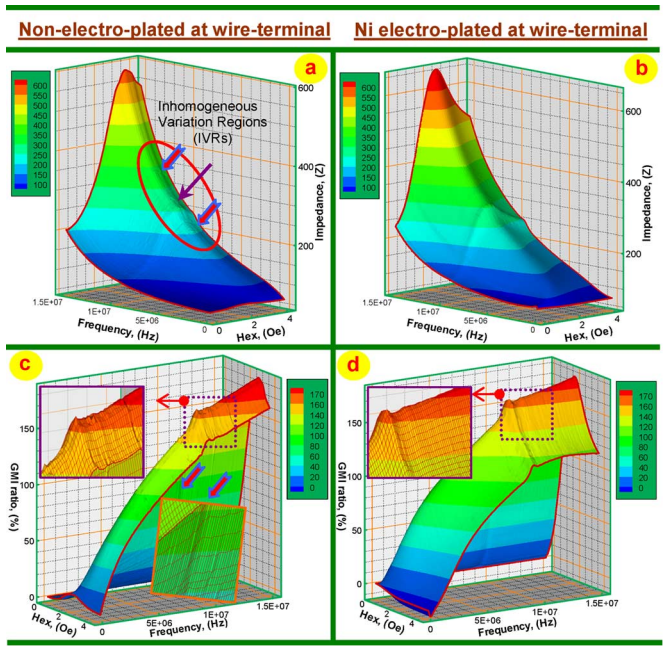

Fig. 6. (a) and (b) Impedance output stabilities and (c) and (d) corresponding GMI ratio $\Delta Z/Z_0$ output stabilities versus frequency (0.1–15 MHz) and magnetic field. The red ellipses indicate the inhomogeneous variation regions (IVRs) of impedance output. The partial mesh magnifications (imaginary purple line) in (c) and (d) are shown in order to illustrate the variation in GMI ratios with increasing applied field (0 Oe–4.25 Oe) at different frequencies, and the uni-direction arrows in (c) indicate the other partial magnification of inhomogeneous GMI variation region between 11.0 and 12.5 MHz.

interface reaction which generates the intermetallic compound $((\mathrm{Cu,Ni})_6\mathrm{Sn}_5)$ in wire-joining process [12].

The microwire with nickel electro-plated two-terminal ends is connected into PCB test board, placed in magnetically shielded space (MSS) to avoid the disturbance by geomagnetic and other magnetic field, for further analysis of the GMI output stability accurately at the same ambient temperature (25 °C) and the pumping current amplitude (20 mA) [19]. The external magnetic field is supplied by a precision solenoid with the high-resolution (0.1 nT) and the maximum magnetic field (4.25 Oe). The impedance and the corresponding GMI output stabilities dependence on the magnetic field (0–4.25 Oe) in the frequency range of 0.1–15 MHz are shown in Fig. 6.

For nonelectro-plated microwires [as shown in Fig. 6(a) and (c)], the impedance variation has some obvious inhomogeneous variation regions (IVRs) from 8 to 12 MHz, especially near 10 MHz. According to GMI ratio output variation, the impedance fluctuation almost runs through all IVRs. The magnified meshes in IVRs magnifications [as shown in Fig. 6(c)] show the obviously flectional variation, this phenomena is almost consistent with the previous reports [20]. For nickel electro-plated at wire-terminal [as seen in Fig. 6(b) and (d)], in contrast to (a) and (c), the IVRs reduce, which improved to some extent, the impedance and corresponding GMI output stability (i.e., similarly as impedance output stability, it can be calculated the variation of GMI ratio according to the impedance output values, exhibiting macroscopic fluctuant variation with increasing magnetic field at different frequency) vary smoothly with the magnetic field and frequency increase, even at relatively high frequency ($f \geq 10$ MHz), thus the GMI output stability is higher than that of nonelectro-plated microwire. The maximum GMI ratio $[\Delta Z/Z_0]_{\max}$ is up to 180.5% at 15 MHz. In fact, nickel electro-plating at wire-terminal is an employed approach to enhance the GMI output stability of microwires. In a word, the electro-plated nickel layer is a good conductor with better wettability interconnecting to SAC. As a result, it reduces the contact resistance of pan weld, and helps to achieve stable wire-connecting. Meanwhile, this type wire-connecting also can avoid the influence of stray and parasitic capacitance in the pan weld and reduce the emission of RF electromagnetic wave and driving signal attenuation, more importantly, suppress destabilization and concussion resulting from contact instability of wire-connecting ends especially at very high frequency. In comparison with our previous report [10], wire-connection by Ni electro-plating also can improve the impedance and GMI output stability, which is similar to the results of Cu electro-plating. The most plausible reason is the stable wire-connection of both two-type electroplatings. On the one hand, the thickness and length of Ni layer at wire-terminal is smaller, only about 2.59 μm and 4 mm, respectively. On the other hand, even though the Ni layer has weak magnetic property, and it has the slight effect on GMI output stability, for the Ni electro-plated wire-terminal was closely wrapped by SAC solder.

Moreover, the former mentioned phenomenon of impedance fluctuation of nonelectro-plated microwire in Fig. 6(a) and (c) also can be explained through the following analogue electronic signal perspective. In the impedance measurement circuit, the pan welds have small physical dimension and electrode area because of the bad wire-combination between nonelectro-plated

wire-terminal and SAC solder, which can be considered as one flat capacitor (C), and if combined with other elements of the branch circuit resistance (R) and inductance (L) of microwire, RLC parallel resonant circuit is formed. In RLC parallel resonant circuit (PRC), the parallel resonance frequency, $f_{\rm p}$, and the value of equivalent impedance Z can be expressed as [21]

$$\begin{cases} f_p \approx \frac{1}{2\pi\sqrt{LC}} \\ Q = \frac{\omega_0 L}{R} \approx \frac{1}{R}\sqrt{\frac{L}{C}} \\ |Z_p| = R + Q^2 R = R + \frac{L}{RC}, \quad (f = f_p) \\ |Z_p| \approx Q^2 R = \frac{L}{RC}, \quad (Q \gg 1) \end{cases} \tag{6}$$

where C is the flat capacitor of the pan weld, with the value of about several hundreds pF; R is the total resistance, including the resistance of microwire and the equivalent loss resistance of inductance and capacity; and L is the inductance of microwire, $L \approx 4 \times 10^{-7}$ H; Q is quality factor of PRC; ω_0 is the angular frequency.

According to the expression (6), the value of $f_{\rm p}$ is in the range of 10.5–14.5 MHz. If the pumping frequency, f, is less than the parallel resonance frequency, $f_{\rm p}$, namely $f < f_{\rm p}$, RLC-PRC circuit has good frequency stability, and it takes on characteristics of an inductive circuit. While if f is near $f_{\rm p}$ $(f \approx f_{\rm p})$, the typical resonance phenomenon occurs obviously, and the impedance value $(/Z_p/ \approx L/RC)$ exhibits dramatic variation, which results in fluctuation of the impedance output. However, for $f > f_{\rm p}$, RLC-PRC circuit takes on characteristics of a capacitive circuit, and the equivalent impedance value of $/Z/$ decreases, and the impedance variation becomes stable again. Thus, it can be inferred that wire-connecting with Ni electro-plating at wire-terminal (at current intensity of 4.0 A/dm^2 for 230 s) could be also a promising choice for EP of GMI and GSI magnetic sensors [22].

IV. Conclusion

In summary, the wire-connecting with Ni electro-plating can significantly stabilize the GMI output of melt-extracted Co-rich amorphous microwires. A uniform and dense pyramid structure of Ni electro-plating layer can be obtained at 4.0 A/dm^2 for 230 s, correspondingly the layer has smaller contact angle (54.60°), making the microwire exhibits better wettability, weldability and impedance output. Compared with nonelectro-plated wire-terminals, Ni electro-plated wire-connecting can reduce the fluctuation of impedance and enhance effectively the GMI output stability at different magnetic field and relatively high frequency $(f \approx f_{\rm p})$. This is of significant importance for the development of high performance and small-sized magnetic and stress-sensing sensors.

References

[1] M. Vázquez and A. Hernando, "A soft magnetic wire for sensor applications," *J. Phys. D: Appl. Phys.*, vol. 29, pp. 939–949, Apr. 1996.

[2] J. Fan, J. Wu, N. Ning, H. Chiriac, and X. Li, "Magnetic dynamic interaction in amorphous microwire array," *IEEE Trans. Magn.*, vol. 46, no. 6, pp. 2431–2434, Jun. 2010.

[3] M. H. Phan and H. X. Peng, "Giant magnetoimpedance materials: Fundamentals and applications," *Prog. Mater. Sci.*, vol. 53, pp. 323–420, Feb. 2008.

[4] F. X. Qin, H. X. Peng, L. V. Panina, M. Ipatov, V. Zhukova, A. Zhukov, and J. Gonzalez, "Smart composites with short ferromagnetic microwires for microwave applications," *IEEE Trans. Magn.*, vol. 47, pp. 4481–4484, 2011.

[5] H. Chiriac and T.-A. Óvári, "Novel trends in the study of magnetically soft Co-based amorphous glass-coated wires," *J. Magn. Magn. Mater.*, vol. 323, pp. 2929–2940, Dec. 2011.

[6] L. V. Panina, S. I. Sandacci, and D. P. Makhnovskiy, "Stress effect on magnetoimpedance in amorphous wires at gigahertz frequencies and application to stress-tunable microwave composite materials," *J. Appl. Phys.*, vol. 97, p. 013701, Jan. 2005.

[7] F. X. Qin and H. X. Peng, "Ferromagnetic microwires enabled multifunctional composite materials," *Prog. Mater. Sci.*, 2012, 10.1016/j.pmatsci.2012.06.001.

[8] H. Hauser, L. Kraus, and P. Ripka, "Giant magnetoimpedance sensors," *IEEE Instrum. Meas. Mag.*, pp. 28–32, Jun. 2001.

[9] T. Y. Tee, H. S. Ng, D. Yap, X. Baraton, and Z. Zhong, "Board level solder joint reliability modeling and testing of TFBGA packages for telecommunication applications," *Microelectron. Rel.*, vol. 43, pp. 1117–1123, Jul. 2003.

[10] Z. W. Zhong, H. M. Ho, Y. C. Tan, W. C. Tan, H. M. Goh, B. H. Toh, and J. Tan, "Study of factors affecting the hardness of ball bonds in copper wire bonding," *Microelectron. Eng.*, vol. 84, pp. 368–374, Feb. 2007.

[11] J. S. Liu, J. F. Sun, D. W. Xing, X. Xue, S. L. Zhang, H. Wang, and X. D. Wang, "Experimental study on the effect of wire bonding by Cu electroplating on GMI stability of Co-based amorphous wires," *Phys. Status Solidi A*, vol. 208, pp. 530–534, Mar. 2011.

[12] A. Zribi, A. Clark, L. Zavalij, P. Borgesen, and E. J. Cotts, "The growth of intermetallic compounds at Sn-Ag-Cu solder/Cu and Sn-Ag-Cu solder/Ni interfaces and the associated evolution of the solder microstructure," *J. Electron. Mater.*, vol. 30, pp. 1157–1164, Jun. 2001.

[13] K. J. Zeng, V. Vuorinen, and J. K. Kivilahti, "Interfacial reactions between lead-free SnAgCu solder and Ni (P) surface finish on printed circuit boards," *IEEE T. Electron. Pack.*, vol. 25, pp. 162–167, Jul. 2002.

[14] Z. Ning, Y. He, and W. Gao, "Mechanical attrition enhanced Ni electroplating," *Surf. Coat. Technol.*, vol. 202, pp. 2139–2146, Sep. 2008.

[15] D. B. George, *Nickel Electroplating, ASM Handbook*. Chicago, IL: ASM International Materials Park, 1994, pp. 201–226.

[16] J. S. Liu, X. D. Wang, F. X. Qin, F. Y. Cao, D. W. Xing, H. X. Peng, X. Xue, and J. F. Sun, "GMI output stability of glass-coated Co-based microwires for sensor application," *PIERS Online*, vol. 7, pp. 661–665, Nov. 2011.

[17] J. Hu, Y. Wang, J. Chen, H. Qin, and B. Li, "Giant magnetoimpedance and colossal ac magnetoresistance of a Cu coil wound on $La_{0.67}Sr_{0.33}MnO_3$," *Solid State Commun.*, vol. 151, pp. 47–50, Oct. 2011.

[18] J. C. Lin, S. B. Jang, D. L. Lee, C. C. Chen, P. C. Yeh, T. K. Chang, and J. H. Yang, "Fabrication of micrometer Ni columns by continuous and intermittent microanode guided electroplating," *J. Micromech. Microeng.*, vol. 15, pp. 2405–2413, Apr. 2005.

[19] J. F. Sun, J. S. Liu, D. W. Xing, and X. Xue, "Experimental study on the effect of alternating-current amplitude on GMI output stability of Co-based amorphous wires," *Phys. Status Solidi A*, vol. 208, pp. 910–914, Apr. 2011.

[20] V. Popov, V. Zhukova, M. Ipatov, C. García, J. Gonzalez, V. Ponomarenko, V. Berzhansky, D. Vinogorodsky, and A. Zhukov, "Studies of giant magnetoimpedance effect of Co-rich microwires in wide frequency range," *Phys. Status Solidi A*, vol. 206, pp. 671–673, Feb. 2009.

[21] S. B. Tong and C. Y. Hua, *Foundation of Analogue Electronic Technology (4th Edition)*. Beijing, China: Higher Education, 2006, pp. 391–405.

[22] J. S. Liu, J. F. Sun, D. W. Xing, and X. Xue, "Twin-detector sensor of Co-rich amorphous microwires to overcome GMI fluctuation induced by ambient temperature," *IEEE Trans. Magn.*, vol. 48, no. 9, pp. 2449–2454, Sep. 2012.

Jing-Shun Liu received the Ph.D. degree in materials processing engineering from the Harbin Institute of Technology, Harbin, China, in 2013, and is currently working toward GMI effect, GMI measurement, and GMI sensor applications of Co-based amorphous microwires.

He is a Lecturer with Inner Mongolia University of Technology, Hohhot, China. In 2009, he joined the Rapid Solidification Technology and Novel Materials (RSTNM) Laboratory.

Da-Wei Xing received the Ph.D. degree in materials processing engineering from the Harbin Institute of Technology, Harbin, China, in 2006.

He has been an Associate Professor with the Harbin Institute of Technology since 2006. His research interests include magnetic properties of bulk metallic glass (BMG), microwave absorption and electromagnetic shielding of ferromagnetic materials and their potential applications.

Da-Yue Zhang received the Master's degree in materials processing engineering from the Harbin Institute of Technology, Harbin, China, in 2011, and is currently working toward the Ph.D. degree in metallurgy and materials at the University of Birmingham, Birmingham, U.K.

Fu-Yang Cao received the Ph.D. degree in materials processing engineering from the Harbin Institute of Technology, Harbin, China, in 2003.

He has been an Associate Professor with the Harbin Institute of Technology since 2004. His research interests include spray forming technique and numerical simulation of Al alloys.

Xiang Xue received the Ph.D. degree in materials processing engineering from the Technical University of Denmark, Copenhagen, Denmark, in 1992.

He has been a Professor with the Harbin Institute of Technology, Harbin, China, since 2002. His research interests include solidification and numerical simulation of superalloys and potential technique applications.

Jian-Fei Sun received the Ph.D. degree in materials processing engineering from the Harbin Institute of Technology, Harbin, China, in 1999.

He has been a Professor at Harbin Institute of Technology since 2003. In 2000, he founded the Rapid Solidification Technology and Novel Materials (RSTNM) Laboratory. His research interests include bulk metallic glass (BMG), characterization and mechanical properties of nanocrystalline and amorphous alloys, and technique applications of functional materials, especially GMI sensor applications.